Solitary-wave propagation in the three-dimensional lattice

Jad H. Batteh and John D. Powell
U.S. Army Ballistic Research Laboratory, Aberdeen Proving Ground, Maryland 21005
(Received 5 February 1979)

The properties of solitary waves in a three-dimensional monatomic face-centered-cubic lattice are studied. The atoms of the lattice are assumed to interact via a Morse-type interatomic potential. For the discrete lattice, the equations of motion for the atoms are solved numerically using a computer-molecular-dynamic technique and, from their solution, the stability of the waves investigated. It is pointed out that the solitary waves are fairly stable to longitudinal planar oscillations, somewhat less stable to mutual collisions, and still less stable to transverse planar oscillations. It is also observed that under some conditions coupled longitudinal and transverse solitary waves can propagate in phase with the same propagation velocity in the lattice. The equations of motion are then derived in the long-wavelength continuum limit and studied in some detail. A comparison of their solutions is made with the results for the discrete-lattice model and it is shown that the continuum equations are capable of predicting many of the same effects.

I. INTRODUCTION

In this paper we will be concerned with studying the propagation and interaction of solitary waves in a face-centered-cubic (fcc) lattice. Our intention will be to determine the extent to which the properties of these waves, well known in many one-dimensional models, are affected by the additional space dimensions and to assess the likely physical implications of these properties. Most of the work will be undertaken using a computer-molecular-dynamic model, although extensive analytic work is also presented.

Since the discovery[1] that solitary-wave solutions of the Korteweg–de Vries (KdV) equation were stable to mutual collisions, these stable pulses (solitons) have received considerable attention. Interest in the problem arises from the fact that, if relatively stable pulses exist in real physical systems, they will substantially affect the manner in which energy is transported in the system as well as the speed with which it approaches thermal equilibrium. Early work[2] on solitons was devoted to the study of one-dimensional systems whose equations of motion could at least be approximated by equations which possessed soliton solutions. More recently, some progress[3–6] has been made in extending the results to multiple dimensions, although the work is largely mathematical in nature and/or applicable to only rather idealized systems. In more applied work, Schneider, Stoll, and Hiwatari[7] have observed in a three-dimensional discrete-lattice model that heat pulses exhibited solitonlike properties, and Ikezi[8] has experimentally verified the existence of solitons in plasmas. These latter results suggest that soliton propagation may indeed be an important real effect in solids and further studies are appropriate at this time.

Our motivation for investigating the particular problem of solitary waves in the fcc lattice arose from our efforts to explain anomalous effects observed in computer simulations of shock waves in discrete lattices. Three-dimensional studies of this problem reported by Tsai and co-workers[9] over the last decade have suggested that the shock profile is not steady in time and that the lattice does not immediately attain thermal equilibrium behind the shock front. Similar results[10–14] have since been reported in one-dimensional models and explained on the basis of solitary-wave propagation. It remains to determine whether the same effects are responsible for the unexpected results in three dimensions. We will address this problem in subsequent work and, for the present time, confine our attention simply to the properties of solitary waves. Specific points discussed include the extent to which the fcc lattice can support solitary waves; the effect of mutual collisions upon the wave profile; the stability of the profiles to perturbations in the direction of propagation as well as perpendicular to it; and the extent to which longitudinal and transverse oscillations are coupled and how the energy is exchanged between them.

We begin in Sec. II by describing the model under consideration, writing down the equations of motion for each atom in the lattice, and describing the method for solving them. In Sec. III we present the results of the numerical studies which have been undertaken using the discrete-lattice model. In particular, we address the generation of solitary waves and discuss their stability. It is pointed out that in some cases it is possible to generate coupled longitudinal and transverse solitary waves which propagate in phase at the same velocity. In Sec. IV we derive the long-wavelength (continuum) limit of the equations

of motion for the fcc lattice. It is demonstrated that there exists a steady solution to the two equations and the solution predicts the coupled solitary waves found in Sec. III. The equations are solved numerically and an approximate analytic solution is also obtained. Finally, Sec. V contains a summary of the results and the conclusions drawn as well as some discussion of the physical implications that the existence of solitary waves might have on energy transfer in crystalline solids.

II. MODEL AND EQUATIONS OF MOTION

The model whose properties we wish to study consists of a pure, monatomic, fcc lattice which is made as long as necessary in the z direction and which is periodic in the x and y directions. The periodicity in these directions is characterized by the integers L_x and L_y, respectively. Thus, for any function F which depends upon the velocities and displacements of the atoms in the lattice we have

$$F(x+lL_xa_0,\ y+mL_ya_0,z)=F(x,y,z)\ , \qquad (2.1)$$

where l and m are arbitrary integers and a_0 is the lattice constant or cube edge of the conventional cell.

The atoms will be assumed to interact via a Morse-type interatomic potential and therefore the Hamiltonian of the lattice can be written

$$H=\frac{1}{2}\sum_{i,\alpha}\vec{v}_{i,\alpha}^{\,2}+\frac{1}{2}\sum_{\substack{i,\alpha\\ j,\beta}}(e^{-R(A_0|\vec{r}_{i,\alpha}-\vec{r}_{j,\beta}|-1)}-1)^2\ . \qquad (2.2)$$

In writing Eq. (2.2) we have adopted the convention whereby the notation (i,α) denotes the αth particle in the ith plane normal to the z axis. These planes are numbered consecutively beginning with the first located at $z=0$. Any convenient labeling scheme may be used to number atoms within a given plane, but the particular convention used is irrelevant to further discussion here. This labeling convention is convenient for some of our later discussions.

In Eq. (2.2) all quantities have been made nondimensional. H represents, of course, the total energy in the lattice and has been normalized by D, the dissociation energy of a single, isolated atom pair; $\vec{v}_{i,\alpha}$ is the velocity of the (i,α)th atom, normalized by $(D/m)^{1/2}$, where m is the atomic mass; $\vec{r}_{i,\alpha}$ is the position vector of the (i,α)th atom, normalized by a_0; A_0 is the lattice constant, normalized by r_0, the separation of an isolated atom pair at minimum potential; and R is a dimensionless parameter representing the degree of nonlinearity in the Morse potential. The sum over (i,α) runs over all atoms in the lattice and that over (j,β) is taken over all atoms in the vicinity of the (i,α)th for which the potential interaction is appreciable.

The equation of motion satisfied by the (i,α)th atom can be found in a straightforward manner from Eq. (2.2) and the result is

$$\ddot{\vec{r}}_{i,\alpha}=2RA_0\vec{F}_{i,\alpha}\ , \qquad (2.3)$$

where $\vec{F}_{i,\alpha}$ is the nondimensional force (normalized by $2RD/r_0$) exerted on the (i,α)th atom by the remaining atoms in the lattice. Explicitly, $\vec{F}_{i,\alpha}$ is given by

$$\vec{F}_{i,\alpha}=\sum_{\beta,j}(e^{-2R(A_0|\vec{r}_{i,\alpha}-\vec{r}_{j,\beta}|-1)}-e^{-R(A_0|\vec{r}_{i,\alpha}-\vec{r}_{j,\beta}|-1)})\frac{\vec{r}_{i,\alpha}-\vec{r}_{j,\beta}}{|\vec{r}_{i,\alpha}-\vec{r}_{j,\beta}|} \qquad (2.4)$$

and each dot represents differentiation with respect to the dimensionless time τ, i.e., the real time normalized by $(m/D)^{1/2}a_0$.

In all our calculations we will be concerned with solving Eq. (2.3) numerically to determine the temporal evolution of the position and velocity of each atom in the lattice subject to some specific set of initial and boundary conditions. From the solution of these equations, it is then possible to infer all information concerning the response of the lattice to any excitation. The procedure for solving Eqs. (2.3) is to employ a fourth-order Runge-Kutta technique.[15] The details of the method of solution, as well as a listing of the appropriate computer program, will be presented elsewhere[16] and will not be discussed further here.

III. NUMERICAL RESULTS FOR DISCRETE LATTICE

In all solutions of Eqs. (2.3) we have, unless otherwise stated, chosen the anharmonicity factor R to be 6.29, a value which leads to a reasonable representation for a lattice of nickel atoms.[17] Furthermore, we have assumed that only atoms which were separated by a distance of unity or less (real distance normalized by a_0) exerted an appreciable force on one another. This assumption is equivalent to assuming that, in the equilibrium lattice, only an atom's first and second nearest neighbors contribute significantly to its potential interaction. The assumption was found to be reasonable for the currently used value of R. The lattice constant A_0 was then calculated[16] so as to minimize the potential and found to be 1.4034.

A. Generation and collision of solitary waves

In previous work we have used the model described in this paper to study shock propagation in solids. In those studies, we observed that, when the atoms of the lattice are initially at rest in their equilibrium positions, compression along a crystalline axis produces a sequence of solitary waves which pro-

pagate into the lattice. The solitary-wave profiles used in the computer experiments which are described in this paper were obtained by isolating a single solitary wave from this sequence.

An example of the shock-wave calculation is shown in Fig. 1. For this case, the end-most plane of the lattice, located at $z=0$, was driven at a nondimensional velocity $U_p=1.0$ in the z direction. The equations of motion of the atoms in the lattice were solved and the velocity-time trajectories of various planes parallel to the plane at $z=0$ were plotted. For this calculation and for all others where the motion of each atom in a plane is identical, the same results are obtained regardless of L_x and L_y, the periodicity of the lattice in the x and y directions. Therefore, L_x and L_y can both be set to unity so that we need to solve the equations of motion for only two atoms in each plane, one located at the corner of the plane and one located at the center.

In Fig. 1 is plotted the z component of the velocity as a function of time τ for the 40th and 80th planes in the lattice. (The single subscript is used hereafter to refer to the plane as a whole.) In order to facilitate comparisons of the graphs, we have plotted the velocity in each case as a function of $\tau-\tau_0$ where τ_0 is the time at which the propagating disturbance first excites the plane in question. It is evident from the figure that a spectrum of solitary waves is evolving near the front of the disturbance, just as occurs in one dimension. Asymptotically, the pulses will completely separate, approach the same constant shape, and propagate at a steady speed through the lattice. Consequently, a single solitary wave can be launched into a lattice by driving the end-most plane with the solitary-wave profile obtained from the shock-wave calculations. This is not the only conceivable method of generating solitary waves in the lattice, but is a reasonable one.

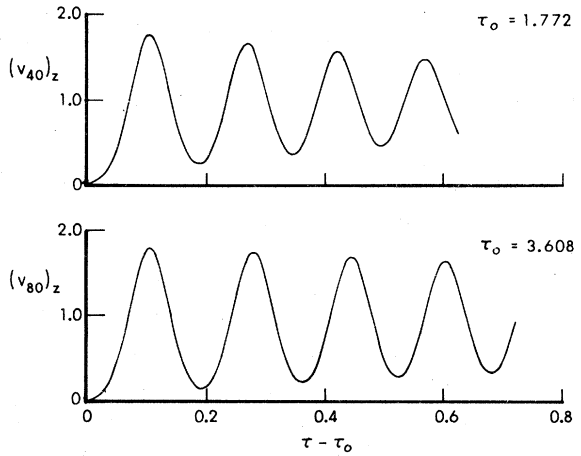

FIG. 1. Spectrum of solitary waves generated by steady compression at rate $U_p=1.0$.

In previous studies[13] we demonstrated that solitary waves propagating in a one-dimensional, Morse-potential lattice are stable to mutual collisions. That is, to within the accuracy of our numerical data, two solitary waves emerged from a collision with the same profile as prior to the collision. It is of interest to determine whether similar effects occur in the three-dimensional, fcc lattice.

We have launched two solitary waves having equal but oppositely directed velocities from opposite ends of a lattice and allowed them to approach one another and eventually collide. By plotting the velocity-time trajectories of various planes encountered by the solitary waves, the effect of the collision can be ascertained. The results of such a calculation are shown in Fig. 2 for two solitary waves launched from the ends of a lattice which was 48 planes long. The initial solitary-wave profiles were obtained from a shock-wave calculation with $U_p=3.0$. The top figure shows the velocity-time trajectory of the 13th plane in the lattice beginning at the time when the solitary wave propagating in the positive z direction first encounters the plane. For the time shown in this figure the two waves have not yet collided so that this profile corresponds to the initial solitary-wave profile. The solitary wave depicted in the figure represents a rather strong disturbance. In fact, in the neighborhood of the solitary wave the density in the lattice is increased by about 40%. The two solitary waves encounter one another in the vicinity of the 24th plane

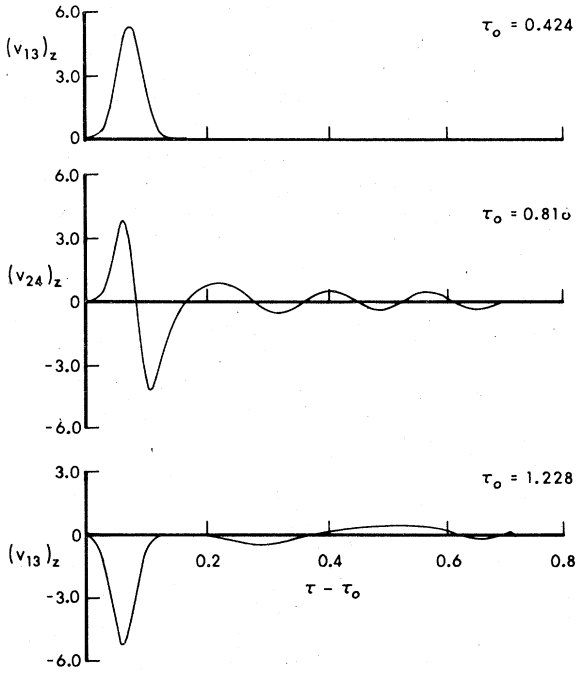

FIG. 2. Collision of two solitary waves.

in the lattice and the trajectory of that plane is shown in the center of the figure during the time of collision. Finally, at a much later time, the collision has been completed and the negative-velocity solitary wave has reached the 13th plane. Its trajectory is shown in the bottom of the figure.

It is apparent from the figure that the two solitary waves maintain their shapes only approximately after the collision. Evidently, some of the energy which initially resided in the two solitary waves now exists in the form of oscillations which are left behind by the waves. Although it is not apparent from the figure, the amplitude of the solitary waves subsequent to the collision is decreased by about 3% from the amplitude prior to the collision. We conclude, then, that solitary waves in an fcc lattice with a Morse-potential interaction are not stable to mutual collisions.

In addition to the results discussed above, we have also observed collisions between solitary waves having smaller initial amplitudes. As the amplitude decreases, the waves appear to become more stable. In fact, solitary waves generated by steady compression with $U_p = 1.0$, having initial amplitudes of about 1.8 (as compared with about 5.4 for the $U_p = 3.0$ case), were found to be stable to within our numerical accuracy.

It might appear surprising that, although the only motion in the fcc lattice is one dimensional, the solitary waves do not appear to be so stable as in our previous one-dimensional chain calculations. The reason for the apparent anomaly is not completely clear but two possible explanations may be offered. First, it must be understood that, even though the motion in the Morse-potential fcc lattice is planar and one dimensional, the model is nevertheless different from a one-dimensional chain with a Morse-potential interaction. Consider, for instance, the one-dimensional chain with the atoms initially in their equilibrium positions. As two neighbors approach one another, their force of interaction increases monotonically, reaching a maximum as the separation distance decreases to zero. In the fcc lattice, however, as two neighboring planes approach one another, the force exerted by an atom on its neighbor in an adjacent plane is not in the same direction as that of the planar motion. Therefore, as the planes approach one another, their force of interaction first increases, reaches a maximum value, and then decreases to zero as the planes become coincident. Of course, it would be possible to reproduce the results of the fcc calculation with a one-dimensional chain model by replacing the Morse-potential interaction with another potential defined so as to give the same force as a function of separation distance in the two cases. Second, it is likely that the solitary waves observed in our previous one-dimensional calculation were not rigorously solitons but only appeared to be so to within our numerical accuracy. Thus, after many collisions we would expect that some change in the solitary-wave profile would be observed. In fact, we speculated then that such an effect might be responsible for the apparent tendency for equilibration that was observed far behind the shock front in our one-dimensional lattice.

B. Stability of solitary waves to planar and thermal oscillations

In addition to investigating the effects of mutual collisions upon the solitary-wave profiles, we have also examined the effects of relatively small planar oscillations both along and transverse to the propagation direction. To perform the calculations we launched a solitary wave at the end of the lattice and allowed it to propagate some distance into the interior. At some point ahead of the solitary wave, a few planes in the quiescent lattice were displaced slightly, released, and allowed to oscillate. The solitary wave then eventually passed through the region of the oscillating planes and emerged on the other side. The intention was to determine the effect of the region of planar oscillations on the solitary-wave profile.

An example of the effect of longitudinal planar oscillations is shown in Fig. 3. A solitary wave having

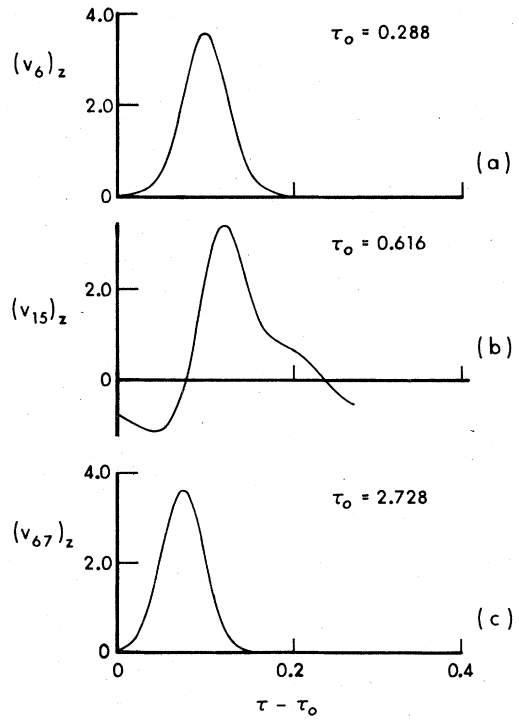

FIG. 3. Effects of longitudinal planar oscillations on solitary-wave profile. (a), (b), and (c) represent solitary wave before, during, and after traversing the oscillatory region, respectively.

an amplitude of 3.6 (generated from compression at $U_p = 2.0$) was launched into the lattice. Just prior to the time the solitary wave reached the 14th plane in the lattice, planes 14–18 were uniformly displaced a distance of 0.1 in the positive z direction and allowed to oscillate. In Fig. 3(a) is plotted the velocity-time trajectory of the 6th plane in the lattice which shows the unperturbed solitary wave. Figure 3(b), on the other hand, shows the same disturbance as it propagates past the 15th plane in the lattice which clearly lies within the region of longitudinal oscillations. The shape of the original solitary wave is obviously distorted as it propagates through the region. Finally, in Fig. 3(c) we have plotted the trajectory of the 67th plane in the lattice at the time when the original disturbance first reaches it. By this time the original solitary wave has completely traversed the region of longitudinal oscillations. Though not shown, the trajectories of some later planes have also been plotted to demonstrate that the shape of the emerging solitary wave did not change.

Comparison of Figs. 3(a) and 3(c) indicates that the longitudinal planar oscillations have had an insignificant effect upon the original solitary-wave profile. In fact, to within our numerical accuracy, the profile was found not to have changed at all. These results might appear surprising since the pulses were found to be unstable to mutual collisions which involve only longitudinal planar oscillations. Apparently, however, the oscillations discussed above were too small a perturbation to make any change in the wave profiles observable numerically. Perhaps if the oscillatory region were much longer, or the oscillations of larger amplitude, a notable effect would have been seen.

Calculations identical to those above, except that the five planes were displaced in the transverse (y) direction, have also been carried out. It is interesting to note that a displacement of the planes in the transverse direction will give rise to both longitudinal and transverse oscillations, whereas displacement in the longitudinal direction produces only longitudinal oscillations. (This point is discussed further later.) Consequently, we cannot examine the stability of the solitary waves to completely transverse oscillations, but only to oscillations which contain a mixture of both. Furthermore, although the planes were displaced by the same amount in the two calculations, the change in the energy in the lattice due to the transverse displacement is approximately a factor of two less than that due to the longitudinal displacement.

The results of propagating the solitary wave through the region containing transverse planar oscillations are shown in Fig. 4. Again, in Fig. 4(a) is shown the unperturbed solitary wave and in Fig. 4(b) the disturbance during the time it traverses the region of planar oscillations. Figure 4(c) represents the

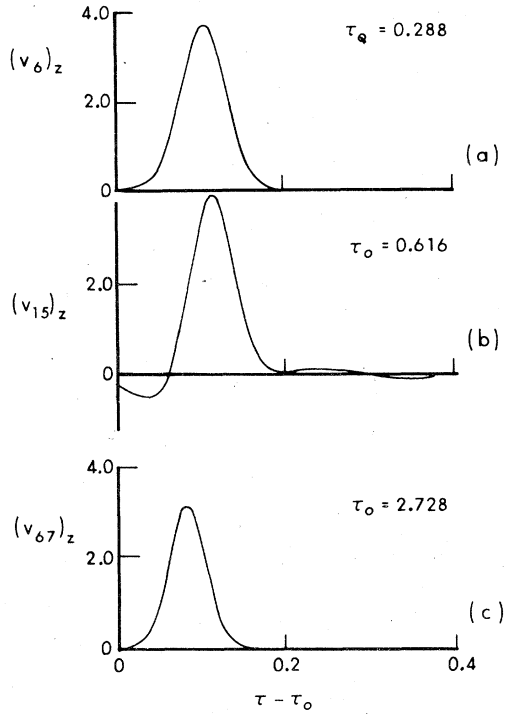

FIG. 4. Effects of transverse and longitudinal oscillations on solitary-wave profile. (a), (b), and (c) represent solitary wave before, during, and after traversing oscillatory region, respectively.

resulting disturbance which emerges from the oscillatory region. As can be seen from the figure, the transverse oscillations have significantly affected the size of the original solitary wave. In fact, the amplitude of the pulse, which was about 3.60 prior to traversing the oscillatory region has been reduced to about 3.12. Again, in order to be certain that the emerging pulse was indeed a solitary wave, we have followed its propagation farther than the 70th plane into the lattice and observed no change in shape.

Finally, we have allowed the solitary wave to propagate through a region which contained random, thermal oscillations. The length of the region was the same as for the previous calculations and the cross section contained 32 atoms ($L_x = L_y = 4$). The thermal energy per particle was the same as the energy per particle associated with the mixture of transverse and longitudinal planar oscillations. Again some decay of the initial solitary-wave amplitude was observed. We should point out, however, that the finite size of the lattice in the transverse directions unavoidably gives rise to some planar oscillations. These planar oscillations, which are unexpected in macroscopic, equilibrated crystals, no doubt accentuate the decay of the solitary-wave profiles. Nevertheless, we expect some decay of the profiles even in the

absence of planar oscillations although the decay should be slower than that observed here. Unfortunately, capability of treating only small systems is a fundamental limitation of computer molecular dynamics.

C. Coupled solitary waves

The instability of the original solitary wave to transverse planar oscillations can be explained in part by the generation of coupled longitudinal and transverse solitary waves. We have observed these waves in the numerical data from which Fig. 4 was plotted. Specifically, it was found that there existed a solitary wave which propagated in phase with the emerging longitudinal wave but which produced a disturbance in the transverse (y) direction.

The effect is demonstrated in Fig. 5 in which we have plotted the velocity-time trajectory of the 70th plane. The upper part of the graph is identical to Fig. 4(c) and represents the emerging longitudinal pulse. On the lower part of the graph is plotted the y component of the velocity of the same plane beginning at the same time. As can be seen from the figure, the transverse solitary wave has somewhat smaller amplitude than the longitudinal wave and propagates in phase with it. We have also computed the energy of the initial-wave profile and compared it with that of the final coupled waves. The final energy was found to be about 10% less in the coupled configuration, suggesting that part of the energy in the initial wave is given up to thermal oscillations.

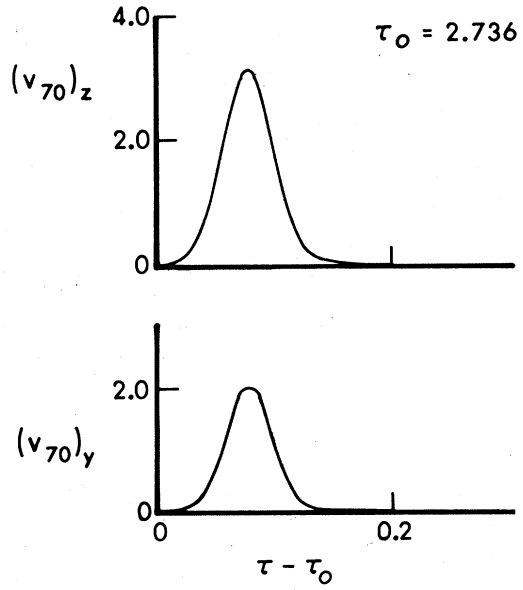

FIG. 5. Coupled longitudinal and transverse solitary waves.

We have also observed coupled solitary waves in our study of the effects of thermal oscillations upon the wave profile. In that case transverse solitary waves were found to propagate in *both* transverse directions. In all likelihood they arose from the planar oscillations generated by the finite size of the crystal discussed earlier. In Sec. IV we will see that the continuum limit of the equations of motion predicts the existence of these coupled solutions and we will discuss their properties in greater detail.

IV. CONTINUUM EQUATIONS

In this section we will derive, interpret, and present some special solutions to the continuum equations for planar oscillations in the fcc lattice. This limit can be expected to be valid whenever the excitations which the equations describe have wavelengths much longer than the interatomic spacing. The purpose of obtaining and solving the equations is to compare the results with those obtained previously for the discrete lattice. As will be seen, the relatively simple continuum equations predict results at least qualitatively similar to those obtained in Sec. III.

A. Derivation of continuum equations for planar oscillations

In order to make the calculations as simple as possible we will assume that only nearest-neighbor interactions are significant. Including more distant neighbors is not expected to affect qualitatively the nature of the results. This is especially true for our case where the anharmonicity factor is rather large. Furthermore, since we are concerned only with planar oscillations, each atom in a plane normal to the z direction will be assumed to have the same velocity and displacement. The velocities and displacements have a y component (transverse) and a z component (longitudinal) but, for simplicity, the x components have been set equal to zero throughout.

We are interested in solving Eq. (2.3), viz.,

$$\ddot{\vec{r}}_{k,\alpha} = 2RA_0 \sum_{j,\beta} \left(e^{-2R(A_0|\vec{r}_{k,\alpha}-\vec{r}_{j,\beta}|-1)} - e^{-R(A_0|\vec{r}_{k,\alpha}-\vec{r}_{j,\beta}|-1)} \right) \frac{\vec{r}_{k,\alpha}-\vec{r}_{j,\beta}}{|\vec{r}_{k,\alpha}-\vec{r}_{j,\beta}|} , \tag{4.1}$$

in the limit in which the displacements of all particles from their equilibrium positions are small. The sum over j and β now runs over the 12 nearest neighbors to particle (k, α) which are shown in Fig. 6.

For the case of planar oscillations, the displacement of particle (k, α) from its equilibrium position is

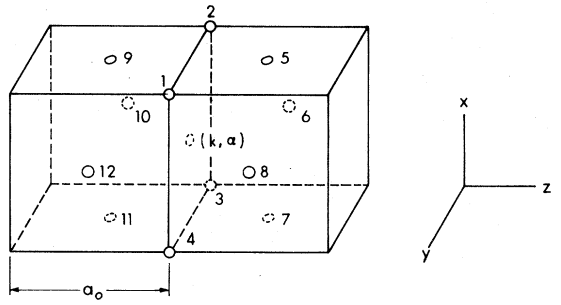

FIG. 6. Location of nearest neighbors to atom (k, α).

TABLE I. Position vectors from lattice site (k, α) to neighboring lattice sites. $\hat{i}$, $\hat{j}$, and $\hat{k}$ are unit vectors in the three Cartesian directions.

Neighbor	$\vec{r}_{j,\beta}{}^0-\vec{r}_{k,\alpha}{}^0$
1	$\frac{1}{2}\hat{i}+\frac{1}{2}\hat{j}$
2	$\frac{1}{2}\hat{i}-\frac{1}{2}\hat{j}$
3	$-\frac{1}{2}\hat{i}-\frac{1}{2}\hat{j}$
4	$-\frac{1}{2}\hat{i}+\frac{1}{2}\hat{j}$
5	$\frac{1}{2}\hat{i}+\frac{1}{2}\hat{k}$
6	$-\frac{1}{2}\hat{j}+\frac{1}{2}\hat{k}$
7	$-\frac{1}{2}\hat{i}+\frac{1}{2}\hat{k}$
8	$\frac{1}{2}\hat{j}+\frac{1}{2}\hat{k}$
9	$\frac{1}{2}\hat{i}-\frac{1}{2}\hat{k}$
10	$-\frac{1}{2}\hat{j}-\frac{1}{2}\hat{k}$
11	$-\frac{1}{2}\hat{i}-\frac{1}{2}\hat{k}$
12	$\frac{1}{2}\hat{j}-\frac{1}{2}\hat{k}$

identical to the displacement of the entire plane k from its equilibrium position. Therefore, we can write

$$\vec{r}_{j,\beta}-\vec{r}_{k,\alpha}=\vec{r}_{j,\beta}{}^0-\vec{r}_{k,\alpha}{}^0+\vec{S}_j-\vec{S}_k \ , \tag{4.2}$$

where the superscript 0 denotes the position vector to the equilibrium position of the particle, and the vectors $\vec{S}_j$ and $\vec{S}_k$ are the displacements of planes j and k, respectively, from their equilibrium positions. The position vectors joining the equilibrium site of atom (k, α) with those of its 12 nearest neighbors are given in Table I.

If we now substitute Eq. (4.2) into Eq. (4.1), expand the resulting equation, and retain only terms through second order in $\vec{S}$, we obtain

$$\ddot{\vec{S}}_k=4R^2\sum_{\beta,j}((\vec{r}_{j,\beta}{}^0-\vec{r}_{k,\alpha}{}^0)\{2(\vec{r}_{j,\beta}{}^0-\vec{r}_{k,\alpha}{}^0)\cdot(\vec{S}_j-\vec{S}_k)+(\vec{S}_j-\vec{S}_k)^2-6(1+R)[(\vec{r}_{j,\beta}{}^0-\vec{r}_{k,\alpha}{}^0)\cdot(\vec{S}_j-\vec{S}_k)]^2\}$$
$$+2(\vec{S}_j-\vec{S}_k)(\vec{r}_{j,\beta}{}^0-\vec{r}_{k,\alpha}{}^0)\cdot(\vec{S}_j-\vec{S}_k)) \ . \tag{4.3}$$

In deriving Eq. (4.3) we have noted that, for nearest-neighbor interactions only, the lattice constant A_0 is given by $\sqrt{2}$.

We now perform the sum in Eq. (4.3) using the values of the equilibrium position vectors given in Table I. After much tedious algebra, we obtain the following equations for the transverse and longitudinal displacements of the kth plane:

$$(\ddot{S}_k)_y=4R^2\{(S_{k+1}+S_{k-1}-2S_k)_y+(1-3R)[(S_{k+1}-S_k)_y(S_{k+1}-S_k)_z-(S_{k-1}-S_k)_y(S_{k-1}-S_k)_z]\} \ ,$$
$$(\ddot{S}_k)_z=8R^2\{(S_{k+1}+S_{k-1}-2S_k)_z+\tfrac{3}{2}(1-R)[(S_{k+1}-S_k)_z^2-(S_{k-1}-S_k)_z^2]+\tfrac{1}{4}(1-3R)[(S_{k+1}-S_k)_y^2-(S_{k-1}-S_k)_y^2]\} \ . \tag{4.4}$$

In Eqs. (4.4), the subscripts y and z denote the components of the displacement in the y and z directions, respectively. Since we are interested in the case in which the wavelength of the disturbance is much larger than the lattice spacing, we can expand $\vec{S}_{k+1}$ and $\vec{S}_{k-1}$ in a Taylor series about $\vec{S}_k$ with the result that

$$\vec{S}_{k\pm1}-\vec{S}_k=\pm\frac{\partial\vec{S}_k}{\partial k}+\frac{1}{2}\frac{\partial^2\vec{S}_k}{\partial k^2}\pm\frac{1}{3!}\frac{\partial^3\vec{S}_k}{\partial k^3}+\frac{1}{4!}\frac{\partial^4\vec{S}_k}{\partial k^4}\cdots \ . \tag{4.5}$$

Substitution of Eq. (4.5) into Eqs. (4.4) then produces

$$\frac{\partial^2 S_y}{\partial\tau^2}=4R^2\left[\frac{\partial^2 S_y}{\partial k^2}+\frac{1}{12}\frac{\partial^4 S_y}{\partial k^4}+(1-3R)\left(\frac{\partial S_y}{\partial k}\frac{\partial^2 S_z}{\partial k^2}+\frac{\partial^2 S_y}{\partial k^2}\frac{\partial S_z}{\partial k}\right)\right] \ , \tag{4.6a}$$

$$\frac{\partial^2 S_z}{\partial \tau^2} = 8R^2\left[\frac{\partial^2 S_z}{\partial k^2} + \frac{1}{12}\frac{\partial^4 S_z}{\partial k^4} + 3(1-R)\frac{\partial^2 S_z}{\partial k^2}\frac{\partial S_z}{\partial k} + \tfrac{1}{2}(1-3R)\frac{\partial^2 S_y}{\partial k^2}\frac{\partial S_y}{\partial k}\right] , \tag{4.6b}$$

where we have now dropped the subscript k. Terms through fourth order have been retained in obtaining Eq. (4.6).

Equations (4.6) describe the propagation of planar disturbances in the fcc lattice in the continuum limit. Although the result has been obtained for the Morse potential, a similar result can obviously be obtained for any interatomic potential whose associated forces are expanded to second order as in Eq. (4.3). If we neglect third- and fourth-order terms (retain only the first term on the right-hand side of the equations) we obtain simply the linear wave equations. Thus, the longitudinal and transverse sound speeds are given in our normalization by

$$C_l = 2\sqrt{2}R \quad \text{and} \quad C_t = 2R \ . \tag{4.7}$$

That the ratio of these two velocities is given by $\sqrt{2}$ can be inferred from elastic-constant data and the well-known fact that for cubic crystals[18]

$$\frac{C_l}{C_t} = \left[\frac{C_{11}}{C_{44}}\right]^{1/2} . \tag{4.8}$$

The ratio of the elastic constants C_{11}/C_{44} has been shown[17] to approach two in the limit of nearest-neighbor interactions only.

The more interesting effects in Eqs. (4.6), however, are contained in the higher-order terms. The third-order terms represent, to lowest order, the nonlinear effects of the potential whereas the fourth-order terms (linear) account for the dispersive nature of the lattice. It is also clear that if these higher-order terms are retained, Eq. (4.6) predicts that a transverse disturbance cannot propagate in the absence of a longitudinal disturbance. Thus, setting $S_z = 0$ in Eq. (4.6b) leads to only trivial, nonoscillatory solutions for S_y. If, however, one sets $S_y = 0$, a solution for S_z can be found from Eq. (4.6b). Our discrete-lattice results have verified this effect as we pointed out in Sec. III B. In that discussion we noted that displacing planes of atoms in the transverse direction produced both longitudinal and transverse oscillations, but a displacement in the longitudinal direction produced only longitudinal oscillations.

Equations (4.6) are obviously difficult to solve and we will be interested only in obtaining approximate special solutions. Our primary interest will be in using the equations to predict analytically the longitudinal solitary-wave profile and in further studying the properties of the coupled solitary waves discovered in Sec. III.

The equations can be somewhat simplified by noting that solitary waves represent steady, traveling-wave solutions to the equations of motion. Thus, we assume solutions of the form

$$S_y = S_y(k - C\tau) = S_y(\xi) \ , \qquad S_z = S_z(k - C\tau) = S_z(\xi) \ , \tag{4.9}$$

where C is the propagation velocity of the resulting wave form, and substitute into Eqs. (4.6). If we define the components of the planar velocity as

$$u = \frac{\partial S_y}{\partial \tau} \ , \qquad v = \frac{\partial S_z}{\partial \tau} \ , \tag{4.10}$$

Eqs. (4.6) become

$$u'' = \alpha u - 4\beta u v \ , \tag{4.11a}$$

$$v'' = \gamma v - \delta v^2 - \beta u^2 \ . \tag{4.11b}$$

The primes denote differentiation with respect to ξ and the constants are defined as follows:

$$\alpha = 12(C^2/C_t^2 - 1) \ , \quad \beta = 3(3R-1)/C \ , \quad \gamma = 12(C^2/C_l^2 - 1) \ , \quad \delta = 18(R-1)/C \ . \tag{4.12}$$

In Secs. IV B and IV C we obtain and discuss some solutions to Eqs. (4.11).

B. Longitudinal solitary waves

The simplest solution of Eqs. (4.11) results whenever no transverse disturbance exists so that u can be set equal to zero throughout. We then have

$$v'' = \gamma v - \delta v^2 \ . \tag{4.13}$$

If Eq. (4.13) is multiplied by v', it can be integrated twice provided that we require that the function and its derivatives vanish at infinity. Performing the calculation we find

$$v = \frac{3\gamma}{2\delta}\,\mathrm{sech}^2(\tfrac{1}{2}\sqrt{\gamma}\xi) \ . \tag{4.14}$$

In obtaining Eq. (4.14) we have assumed $\gamma > 0$; the solution for $\gamma < 0$ is oscillatory, does not vanish at infinity, and will not be considered here. Analytic

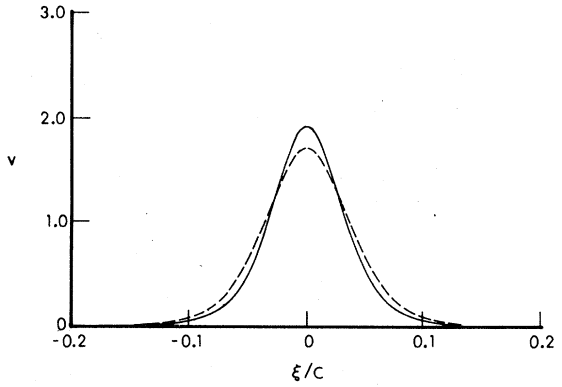

FIG. 7. Comparison of numerical and analytic longitudinal solitary-wave profiles. The dashed curve represents the numerical results for the discrete lattice; the solid curve represents a plot of Eq. (4.14).

approximations for solitary-wave profiles similar to this result have been discussed in the literature.[19]

In order to compare the wave profile predicted by Eq. (4.14) with our numerical data for the discrete lattice, we plotted the velocity-time trajectory of a plane of atoms in the lattice as a solitary wave traversed it. The propagation velocity, C, of the solitary wave was obtained from the computer data and substituted into Eqs. (4.12). The resulting constants were then used to calculate the profile in Eq. (4.14). Results of the calculation are shown in Fig. 7 in which are plotted the numerical and analytic wave profiles as a function of the parameter ξ/C. The two profiles are in reasonably good agreement. We have also compared a number of other profiles for both higher- and lower-amplitude solitary waves. However, as the amplitude of the wave increases, its width decreases. The discrepancy between analytic and numerical results then increases owing to the inadequacy of the continuum approximation.

C. Coupled solitary waves

We now wish to determine whether we can predict from Eqs. (4.11) the coupled longitudinal and transverse solitary waves observed previously. We begin by obtaining an approximate analytic solution to the equations valid in the limit $u \to 0$. The technique may be viewed as the first step in an iterative procedure; in principle, it may be repeated as often as desirable.

Equation (4.14) represents the solution of Eq. (4.11b) for $u=0$. Substituting the result into Eq. (4.11a) we obtain an equation for the first approximation to u, namely,

$$u'' = \alpha u - \frac{6\beta\gamma}{\delta}\,\mathrm{sech}^2(\tfrac{1}{2}\sqrt{\gamma}\xi)\,u \quad . \tag{4.15}$$

Equation (4.15) is linear and second order and is similar to the time-independent Schroedinger equation. Since $\alpha > 0$, one expects[20] that bounded solutions exist only for certain discrete values of C and that the corresponding functions u vanish at infinity.

To solve the equation we make the change of variable

$$y = \mathrm{sech}(\tfrac{1}{2}\sqrt{\gamma}\xi) \tag{4.16}$$

and substitute into Eq. (4.15) to produce

$$\tfrac{1}{4}\gamma y^2(1-y^2)\frac{d^2u}{dy^2} + \tfrac{1}{4}\gamma y(1-2y^2)\frac{du}{dy} = \alpha u - \frac{6\beta\gamma}{\delta}y^2 u \quad . \tag{4.17}$$

We now assume that the solution to Eq. (4.17) can be represented in the form of the series

$$u = \sum_{p=0}^{\infty} u_p y^{m+2p} \quad , \tag{4.18}$$

where m is a positive number, and substitute into Eq. (4.17). Equating coefficients of y^{2l} in the resulting expression then yields the recursion relation

$$u_l = \frac{\gamma(m+2l-2)(m+2l-1) - 24\gamma\beta/\delta}{\gamma(m+2l)^2 - 4\alpha}\,u_{l-1} \quad . \tag{4.19}$$

By assumption $u_0 \neq 0$ so that the denominator of Eq. (4.19) must vanish for $l=0$. Thus, we obtain the eigenvalue equation

$$\tfrac{1}{4}m^2\gamma = \alpha \quad , \tag{4.20}$$

which becomes

$$\frac{C^2}{C_l^2} = \frac{m^2-4}{m^2-8} \tag{4.21}$$

after using Eqs. (4.12). This result indeed predicts that solutions to Eq. (4.17) exist only for certain well-defined values of C. Furthermore, if the series represented by Eq. (4.18) is to terminate, the numerator of Eq. (4.19) must vanish for some value of l. This condition implies

$$m = \tfrac{1}{2}\{-(4l-3) + [1 + 16(3R-1)/(R-1)]^{1/2}\} \quad , \tag{4.22}$$

where all constants have been expressed in terms of R. Of course, m must be greater than zero in order for the solution to remain bounded at infinity.

As a specific example, let us now evaluate the solution for the case $R = 6.29$. In that case, Eq. (4.22) predicts that the only solution which leads to $m > 0$ and $\gamma > 0$ occurs for $l = 1$ and $m = 3.21$. Substitution of m into Eq. (4.21) then yields $C = 1.66 C_l$ and, from this value of C, the remaining constants can be calculated from Eq. (4.12). Only the zeroth

term then survies in the expansion of Eq. (4.18) and we have

$$u = u_0 \operatorname{sech}^{3.21}(2.3\xi) \quad . \tag{4.23}$$

The corresponding expression for v, obtained from Eq. (4.14), is

$$v = 9.8 \operatorname{sech}^2(2.3\xi) \quad . \tag{4.24}$$

In principle, Eq. (4.23) could now be used in Eq. (4.11b) to obtain a second approximation to v.

It is important to emphasize that Eqs. (4.23) and (4.24) represent only a rather crude approximation to Eq. (4.11) which can be expected to be valid only as u tends to zero. The solution predicts, for instance, that the amplitude of the longitudinal solitary wave in the coupled-wave profile is identical to that for an isolated longitudinal wave having the same value of C; actually the amplitude is diminshed from that of the isolated wave. Furthermore, the value of u_0 cannot be obtained in the lowest-order solutions to the equations and this parameter must be fit to the data. Finally, the lowest-order approximation yields only one acceptable eigenvalue and, thus, one solution to the equations. Other solutions are, however, possible as u increases from zero and these are no doubt predicted by higher-order approximations. Despite these shortcomings, the analytic solution is nonetheless valuable because it does predict that coupled-wave solutions do exist and, as we shall see, predicts the shapes of the wave profiles rather well for $u \ll v$.

Because of the limitations of the analytic solution we have also obtained numerical solutions of Eqs. (4.11). Our efforts have been confined to obtaining solutions which propagate in phase, that is, to solutions which reach their maximum at the same value of ξ. Only solutions having this property have been observed in our studies of the discrete-lattice equations. The numerical procedure was as follows: A value for $v_{\max}$ was assumed (arbitrarily chosen at $\xi = 0$) and $u_{\max}$ obtained from the differential equations. Specifically, if we multiply Eq. (4.11a) by u', Eq. (4.11b) by $2v'$, and add the resulting expression is in the form of an exact differential. Integrating and evaluating the resulting equation at $\xi = 0$ yield

$$u_{\max} = v_{\max}\left[\frac{2\delta v_{\max}/3 - \gamma}{\alpha/2 - 2\beta v_{\max}}\right]^{1/2} \quad . \tag{4.25}$$

These values of $u_{\max}$ and $v_{\max}$ were used as initial conditions and a fourth-order Runge-Kutta scheme employed to solve Eqs. (4.11). As expected from the analytic result, the numerical solutions were found to diverge as $|\xi| \to \infty$ unless the appropriate value of C, found by trial and error, was used.

We have performed a number of numerical solutions of Eqs. (4.11) in the manner discussed assuming various values of $v_{\max}$. In no case were we able to obtain convergent solutions for values of $v_{\max}$ less than or equal to the value predicted by the analytic technique in lowest order, namely, $v_{\max} = 9.8$. The result suggests that there exists a threshold, occurring at the eigenvalue $C = 1.66 C_l$, below which the coupled solitary waves cannot propagate in phase. Unfortunately, the threshold is sufficiently high that one cannot expect that the continuum equations are a reasonable quantitative approximation to the discrete-lattice equations and a direct comparison of the results is not possible. Nonetheless, it is interesting that these equations predict both the existence of the coupled waves as well as the fact that they obey a threshold.

An example of a numerical solution is shown by the solid curve in Fig. 8. The solution was obtained by assuming a value of $v_{\max}$ given by 10.24 and was found to converge provided C was given by 29.9 or $1.68 C_l$. A plot of u obtained from the resulting solution is shown in the lower half of the figure; $u_{\max}$ was found to be approximately 1.5 as can be verified from Eq. (4.25).

Since u is considerably less than v one expects that the analytic solution represented by Eqs. (4.23) and (4.24) might well be a reasonable approximation to the numerical result. This is in fact found to be the case as can be seen from the top graph in which the dashed curve represents the solution given by Eq.

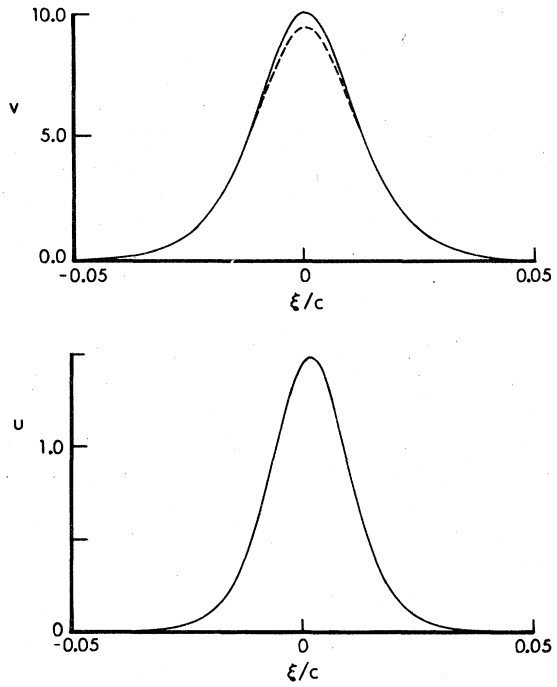

FIG. 8. Comparison of numerical and analytic solutions of Eqs. (4.11). The dashed line represents the analytic solution, the solid line the numerical solution.

(4.24). Furthermore, when we set u_0 in Eq. (4.23) equal to 1.5 and attempted to plot the results on the lower half of the graph along with the numerical solution for u, the graphs were found to be coincident to within the accuracy with which we could plot the data. Consequently, we conclude that the analytic solution is a reasonable approximation to the coupled solitary-wave profile for values of v_{max} near the threshold value of 9.8.

Equations (4.11) merit further study. We have confined our attention in this investigation only to solutions which have their maximum at the same value of ξ. We have been unable to prove from the differential equations, however, that all solutions which vanish at infinity have this property. Thus, although we have not observed it in solutions to the discrete-lattice equations, there remains the possibility that coupled waves exist which propagate out of phase. It is interesting to note that if such solutions exist they too obey a threshold effect, although not necessarily the same one discussed previously. In fact, it is shown in the Appendix that for *all* bounded solutions to Eqs. (4.11), C must obey the condition

$$C > \left(\frac{2R}{1+R}\right)^{1/2} C_l \ . \tag{4.26}$$

For $R = 6.29$, this yields $C > 1.31 C_l$ which is substantially lower than the value $C > 1.66 C_l$ suggested for the in-phase solutions.

V. SUMMARY AND CONCLUSIONS

We have undertaken both computer-molecular-dynamic as well as some analytic studies of solitary-wave propagation in the three-dimensional fcc Morse-potential lattice. It has been found that the lattice is capable of supporting the propagation of solitary waves as in one-dimension. The basic conclusions reached regarding the properties of the solitary waves are as follows: (i) Longitudinal solitary waves are not stable to mutual collisions, the degree of stability decreasing as the amplitude of the colliding solitary waves increases. Nevertheless, even in a mutual collision, which represents a rather strong longitudinal disturbance, the solitary wave retains its integrity fairly well. (ii) The solitary waves are extremely stable to small longitudinal planar oscillations. (iii) Longitudinal solitary waves are not stable to small, transverse planar oscillations. However, even in this case, most of the energy associated with the initial solitary wave remains localized in the form of a coupled longitudinal and transverse solitary wave. (iv) Solitary waves appear to be more stable to random thermal oscillations than to coherent planar oscillations, although it is difficult to determine this conclusively from computer simulations.

Our calculations suggest that, for a variety of perturbations, the energy initially associated with a solitary wave tends to remain localized within the wave, although there may be an exchange of energy between longitudinal and transverse oscillations. Therefore, despite the absence of total stability of the solitary waves, they will nonetheless be important in three-dimensional energy-transport problems. For instance, computer simulations have shown that solitary waves are generated whenever a solid is subjected to shock compression and they will, no doubt, be generated in other nonequilibrium problems as well. Their fair degree of stability, then, insures that solitary waves will substantially affect, at least initially, both the relaxation time and the manner in which thermal equilibrium is re-established after a disturbance. Furthermore, for systems of realistic dimensions which are initially in thermal equilibrium, the solitary waves are likely to be more stable than the calculations reported here suggest because of the absence of coherent planar oscillations in the background.

APPENDIX

The purpose of this Appendix is to prove that for solutions of Eqs. (4.11) which vanish at infinity, the eigenvalues obey a threshold condition. That is, we demonstrate that for solutions of the equations to exist we must have

$$\frac{C^2}{C_l^2} > \frac{2R}{1+R} \ . \tag{A1}$$

Consider Eqs. (4.11), viz.,

$$\begin{aligned} u'' &= \alpha u - 4\beta u v \ , \\ v'' &= \gamma v - \delta v^2 - \beta u^2 \ . \end{aligned} \tag{A2}$$

If the solution for u is to vanish at infinity, then it must have a maximum in a region where u is positive and/or a minimum in a region where u is negative. The final result is independent of which of these situations exists, so let us assume that u has a maximum value u^* at $\xi = \xi^*$, and that $u^* > 0$. Furthermore, let us denote the value of v at ξ^* by v^*. If u is to be a maximum at $\xi = \xi^*$, its second derivative evaluated at ξ^* must be negative. Consequently, from Eq. (A2) we have

$$(\alpha - 4\beta v^*) u^* < 0 \tag{A3}$$

and, since $u^* > 0$,

$$v^* > \frac{\alpha}{4\beta} \ . \tag{A4}$$

If we multiply the first of Eqs. (A2) by u' and the

second by $2v'$, add, and integrate, we obtain

$$\tfrac{1}{2}(u')^2+(v')^2=\tfrac{1}{2}\alpha u^2+\gamma v^2-\tfrac{2}{3}\delta v^3-2\beta u^2 v\geq 0 \ . \tag{A5}$$

We now apply relation (A5) at $\xi=\xi^*$ to produce

$$\tfrac{1}{2}(\alpha-4\beta v^*)u^{*2}+v^{*2}(\gamma-2/3\delta v^*)\geq 0 \ . \tag{A6}$$

Equations (A4) and (A6) imply that v^* must obey the relation

$$\frac{\alpha}{4\beta}<v^*\leq\frac{3\gamma}{2\delta} \ . \tag{A7}$$

In order for a solution to exist, then, we must have that

$$\frac{\alpha}{4\beta}<\frac{3\gamma}{2\delta} \ . \tag{A8}$$

Expressing the constants in terms of C and R [see Eqs. (4.12)] yields finally

$$\frac{C^2}{C_l^2}>\frac{2R}{1+R} \ . \tag{A9}$$

[1]N. J. Zabusky and M. D. Kruskal, Phys. Rev. Lett. 15, 240 (1965).

[2]A. C. Scott, F. Y. F. Chu, and D. W. McLaughlin, Proc. IEEE 61, 1443 (1973).

[3]J. Denavit, N. R. Pereira, and R. N. Sudan, Phys. Rev. Lett. 33, 1435 (1974).

[4]K. H. Spatschek, P. K. Shukla, and M. Y. Yu, Phys. Lett. A 54, 419 (1975).

[5]Y. Gell, Phys. Rev. A 16, 402 (1977).

[6]R. G. Newton, J. Math. Phys. 19, 1068 (1977).

[7]T. Schneider, E. Stoll, and Y. Hiwatari, Phys. Rev. Lett. 39, 1382 (1977).

[8]H. Ikezi, in *Solitons in Action,* edited by K. Lonngren and A. Scott (Academic, New York, 1978), p. 153.

[9]D. H. Tsai, in *Accurate Characterization of the High-Pressure Environment,* edited by E. C. Lloyd, Natl. Bur. Stds. Spec. Publ. No. 326 (U. S. GPO, Washington, D.C., 1971), p. 105.

[10]J. Tasi, J. Appl. Phys. 43, 4016 (1972); see also J. Appl. Phys. 44, 1414(E) (1973).

[11]J. Tasi, J. Appl. Phys. 44, 4569 (1973).

[12]J. Tasi, J. Appl. Phys. 44, 2245 (1973).

[13]J. H. Batteh and J. D. Powell, J. Appl. Phys. 49, 3933 (1978).

[14]J. H. Batteh and J. D. Powell, in *Solitons in Action,* edited by K. Lonngren and A. Scott (Academic, New York, 1978), p. 257.

[15]B. Carnahan, H. A. Luther, and J. O. Wilkes, *Applied Numerical Methods* (Wiley, New York, 1969), Chap. 6.

[16]J. D. Powell and J. H. Batteh, Ballistic Research Laboratory Report, 1979 (unpublished).

[17]F. Milstein, J. Appl. Phys. 44, 3825 (1973).

[18]W. P. Mason, in *American Institute of Physics Handbook,* edited by D. E. Gray (McGraw-Hill, New York, 1957), p. 3-82.

[19]N. J. Zabusky, in *Nonlinear Partial Differential Equations,* edited by W. F. Ames (Academic, New York, 1967), p. 223.

[20]A. Messiah, *Quantum Mechanics* (Wiley, New York, 1966), Vol. 1, Chap. 2.